



## The effect of turbulence on a multi-hole Pitot calibration



Christopher Crowley\*, Iosif I. Shinder, Michael R. Moldover

Sensor Science Division National Institute of Standards and Technology (NIST), 100 Bureau Dr. Gaithersburg, MD 20899, USA

### ARTICLE INFO

#### Article history:

Received 4 December 2012

Received in revised form

23 May 2013

Accepted 28 May 2013

Available online 10 June 2013

#### Keywords:

Airspeed calibration

Multi hole Pitot tube

Detached boundary layer

Turbulence

### ABSTRACT

Accurate calibrations of multi-hole Pitot tubes require thousands of measurements spanning ranges of the fluid's velocity, and the pitch and yaw angles. When calibrating a commercially-manufactured multi-hole Pitot tube in NIST's low-turbulence wind tunnel, we found hysteresis in certain ranges of airspeed, pitch angle, and yaw angle. In the worst case, the hysteresis caused a calibration error of 30%. We demonstrate that the hysteresis was caused by a flow instability associated with flow separation. A turbulence intensity of only 1% removes the hysteresis; however, the calibration depends on the turbulence intensity over the entire range of our measurements (0.25–2%). Therefore, multi-hole Pitot tubes should be calibrated and used at the same turbulence levels.

Published by Elsevier Ltd.

### 1. Introduction

NIST is developing techniques to calibrate 2-D and 3-D anemometer systems, including multi-hole Pitot tubes. One motivation for this project is an emerging need to measure the CO<sub>2</sub> flux (the product of flow rate and CO<sub>2</sub> concentration) in the stack gases emitted by coal-burning power plants with uncertainties on the order of 1%. In 2010, eastern Canada and the northeastern states of the United States agreed to the Regional Greenhouse Gas Initiative (RGGI). This initiative aims to reduce CO<sub>2</sub> emission by 10% by 2018. This goal implies a need for accurate CO<sub>2</sub> flux measurements. Today, CO<sub>2</sub> flux measurements are made in stacks to control the emissions of the pollutants SO<sub>2</sub>, NO<sub>x</sub> and Hg; however, present-day CO<sub>2</sub> flux measurements may have uncertainties in the range 5–10%. [2,3] Reducing these uncertainties may require 2-D or 3-D probes as these devices can account for the large swirl that occur in many power plant stacks. Furthermore, new calibration techniques may be required to calibrate 2-D and 3-D instruments.

One of the most widely used methods for measuring the efflux of greenhouse gasses is a Pitot tube survey of the stack cross-section. The EPA has developed protocols for stack surveys using 1, 2 and 3 dimension static differential pressure devices, such as the standard Pitot static tubes, S-probes and multi-hole pitot tubes. NIST has designed and installed a manual rig for calibrating 2-D and 3-D airspeed instruments in its low-turbulence wind tunnel. In the near future an automated rig will replace the manual one. NIST's first calibration of a five-hole conically-shaped pitot tube

revealed a flow instability that introduced hysteresis into the calibration data. This hysteresis was removed when a sufficient amount of turbulence was introduced into the flow [1]. Here we show that the air-speed calibration in certain yaw and pitch angles is dependent on the turbulent intensity. We anticipate that NIST's low-turbulence wind tunnel will be modified to calibrate pitot tubes used to survey turbulent flows in stacks.

#### 1.1. Multi-hole static Pitot tube

The EPA has approved measurement protocols that use multi-holed pitot tubes to determine the flux of greenhouse gasses and other pollutants emitted into the atmosphere from smokestacks for regulatory purposes. The protocols require measurements of the gas's composition and flow from a stack. Multi-holed, or 3-D, Pitot tubes are used to measure a fluid's velocity, in situations where a 1-D Pitot tube cannot be accurately aligned with the flow. Multi-holed pitot tubes determine the velocity, yaw angle, and pitch angle from measurements of the differential pressure between pairs of holes located near the tip of the sensor [4]. The flow is determined by integrating point velocity measurements made by traversing a multi-holed Pitot tube, along diametric chords of the stack. This method of measuring flux is traceable to SI units through the calibration of the Pitot tube. The pitch and yaw responses of multi-hole pitot tubes are quite complicated; therefore, accurate calibrations require thousands of measured points. Because accurate models do not exist, the calibration data must be disseminated as tables instead of using calibration factors related to dynamic pressure as is done for standard Pitot tubes and for S-probes.

\* Corresponding author. Tel.: +1 301 975 4648.

E-mail address: [Christopher.crowley@nist.gov](mailto:Christopher.crowley@nist.gov) (C. Crowley).

## 2. Calibrations

### 2.1. Airspeed calibration facility

NIST's Dual Test Section Wind Tunnel is a toroid-shaped, closed-loop structure lying in a horizontal plane [5,6]. The wind tunnel has two interchangeable test sections in order to span the airspeed ranges from 0.2 m/s to 75 m/s. Both test sections are 12 m long; however, their cross-sections differ. The high-speed test section – where the 3-D calibrations are conducted – has a height that gradually decreases from 2.1 m to 1.2 m along the flow direction, forming a venturi-like duct. This high-speed test section provides longitudinal free-stream turbulence levels of 0.25% over most of the airspeed range and a transverse velocity gradient of less than 1% within a working area that spans 90% of the test section's cross-section.

Calibrations performed in NIST's wind tunnel are traceable to the SI system through a Laser-Doppler Anemometer (LDA). The LDA is calibrated against a spinning disk primary standard. [5,6]

### 2.2. Calibration rig

The present research used a manually operated calibration rig to manipulate the orientation of the Pitot tube. This rig was attached to the wall of the high-speed section of the wind tunnel. The pitch angle between the Pitot tube and the flow was varied by rotating the instrument under test (IUT) along a flat shelf that ensured the roll angle was fixed. The yaw angle was varied by rotating the IUT inside the mounting clamps. The flat shelf supported the IUT and was marked to measure pitch angles. The yaw angle was measured by a digital inclinometer coupled to the IUT. The uncertainty of yaw and pitch measurements were  $0.1^\circ$  and  $0.2^\circ$  respectively. This calibration rig can be used to calibrate any 3-D anemometer that can be mounted on a rod.

We are developing an automated calibration rig that will replace the manual one. The automated rig will have four degrees of freedom in order to ensure the sensor tip is always at the same location in the wind tunnel.

## 3. Unexpected finding: hysteresis

During a calibration of the cone-shaped, five-hole Pitot tube<sup>1</sup> shown in Fig. 1, we discovered that when the tube was oriented in the range  $20^\circ \pm 5^\circ$  away from the tunnel's axis, strong hysteresis was present in the measured values of pressure differences as the air speed was increased and decreased (See Fig. 2A).

To characterize the hysteresis we define the calibration factor  $C_i$  by the ratio

$$C_i \equiv \Delta P_{\text{IUT},i} / \Delta P_{\text{standard}} \quad (1)$$

The numerator of  $C_i$  is the pressure difference between the center hole and the  $i$ th off-axis hole of the instrument under test (IUT). The denominator of  $C_i$  is the differential pressure measured by a 1-D pitot tube that NIST routinely uses as a check-standard for measurements of air speed. The check standard was located one meter away from the IUT and in the same cross sectional plane of the wind tunnel.

<sup>1</sup> Model DC-250-78.72-J-76.72-CD manufactured by United Sensor Corp., Amherst, N.H. USA. In order to describe materials and procedures adequately, it is occasionally necessary to identify commercial products by manufacturer's name or label. In no instance does such identification imply endorsement by the National Institute of Standards and Technology, nor does it imply that the particular product or equipment is necessarily the best available for the purpose.



Fig. 1. Cone-shaped, five-hole Pitot tube. The diameter of the curved tube is 9.5 mm.

As shown in Fig. 2A,  $\Delta P_{\text{IUT}}$  was smaller when the air speed increased than when the air speed decreased. By exchanging the differential pressure sensors and associated instruments, we verified that the hysteresis did not originate in the pressure instruments. Instead, the hysteresis resulted from the flow interacting with the pitot tube itself. Because the sensing region of the pitot tubes is small, we decided to study the flow around the pitot tube using a fully-functional, scale-model tube that was a factor of 5 larger than the commercially manufactured pitot tube. To match Reynolds numbers, the velocity range was reduced by a factor of 5. As shown in the lower panel of Fig. 2, the model tube (B) and the “real” tube (A) had hysteresis of comparable size at the comparable yaw angles at velocities 1/5th as large as expected from Reynolds scaling. The hysteresis in the model was approximately 10% while the hysteresis in the original tube was approximately 17%. Perhaps this difference resulted from errors in machining the scaled model.

## 4. Investigating the hysteresis

### 4.1. Visualization

To generate smoke streamlines that visualized the flow around the 5X model Pitot tube, a 0.25 mm diameter nickel-chromium wire was installed upstream of the Pitot tube. The wire's diameter was small enough that it did not disturb the flow. Upon command from outside the wind tunnel, a capillary tube dropped “Proto-Smoke<sup>1</sup> fluid” (toy model train smoke oil) near the top of the wire. The oil naturally ran down the wire and beaded up into droplets that became smoke streaks when an electrical current was passed through the wire. To enhance contrast, a black cloth was attached to the wall of the tunnel opposite the camera and back lighting was applied from windows upstream and downstream of the black cloth. Representative pictures are shown in Fig. 3. The photographs revealed a recirculation zone above the hole that exhibited hysteresis that corresponded to the differential pressure measurement. The pressure gradient inside a recirculation zone depends in a complicated way on the flow structure inside the zone. The many aspects of recirculation zones depend nonlinearly on their surrounding conditions and, for this reason, can exhibit hysteretic behavior. All three pictures in Fig. 3 shows flow separation; however picture (A) appears to have more mixing in the recirculation zone. Based on the pictures, the portion of the calibration curve that is discontinuous appears to be linked a more turbulent recirculation zone. With the information gained from the photographs, we began a more quantitative investigation.

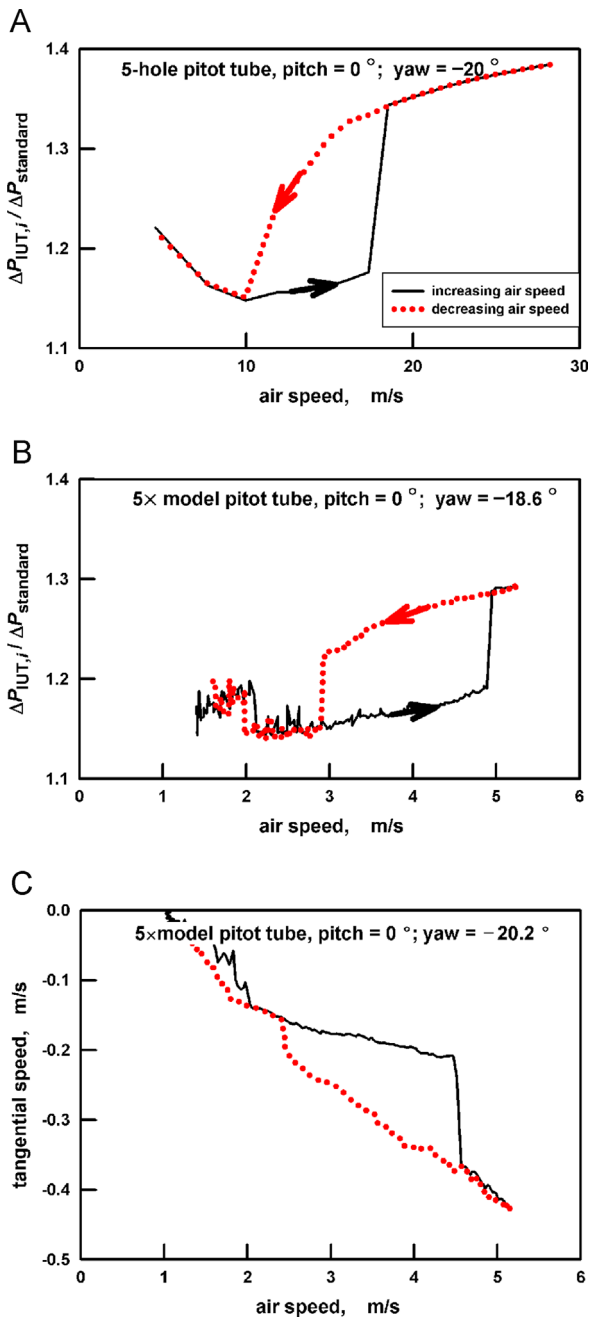


**Fig. 2.** Characterization of observed hysteresis (A) in measured pressure ( $\Delta P_{IUT,i}$ ) of a commercially manufactured five hole Pitot tube, (B) in the measured pressure ( $\Delta P_{IUT,i}$ ) of a five-times-larger model of the five hole Pitot, and (C) the LDA measured tangential air speed 0.03 mm above the surface of the 5X model.

#### 4.2. LDA survey near the Pitot tip

We used a LDA to measure the 3-D velocity profile near the tip of the 5X model. Here, we discuss only the stream wise velocity measured approximately 0.03 mm above the Pitot tube's surface. As shown in Fig. 2C, the tangential velocity exhibits hysteresis in the same range of airspeeds that the differential pressure has hysteresis. Note that the tangential air flow above the surface near the hole is negative and therefore in the direction opposite to the primary flow generated by the tunnel. As the airspeed in the wind tunnel increases, the magnitude of counter-flow slowly increases. At a particular airspeed (4.5 m/s) in Fig. 2C, the flow near Pitot tube's surface undergoes a transition. After this transition occurs, the magnitude of the counter-flow is approximately 85% of the air

speed in the wind tunnel. As the air speed is decreased, the flow structure in this recirculation zone gradually approaches the structure before the transition.

To test the role, if any, played by the holes themselves, we rotated the 5X model by 45°, thereby moving the hole out of the recirculation zone. The counter-flow velocity exhibited the same behavior; therefore, the hysteresis is not caused by the holes but, by the geometry of the Pitot tube itself.

## 5. Turbulence removes hysteresis

### 5.1. Hysteresis depends on turbulence

The hysteresis is caused by a flow transition connected with the recirculation zone. The transition is sensitive to the condition surrounding of the recirculation zone. A light bump of the Pitot tube when the velocity is increasing can cause the transition to occur at a lower velocity. Similarly, by increasing the amount of turbulence present in the wind tunnel, the hysteresis disappears and the shape of the calibration curve in the region near the hysteresis changes.

### 5.2. Generating and quantifying turbulence

To define the percentage turbulence intensity  $T$  in the wind tunnel by the ratio

$$T/(1\%) \equiv 100 \times \text{rms}(v)/\langle v \rangle \quad (2)$$

where the numerator is the root-mean-square (rms) fluctuation of the velocity and the denominator is the average free stream velocity. We measured the rms fluctuations using a commercially-manufactured constant-temperature hot-wire anemometer.

To generate a varying turbulent intensity, we installed a wire mesh on a track upstream of the Pitot tube. We used two different meshes; the first had a wire thickness of 0.58 mm and wire spacing of 2.2 mm resulting in a porosity of 63%. The second mesh had a wire thickness of 0.3 cm and wire spacing of 1.3 cm resulting in a porosity of 65%. The turbulence generated from a mesh has a homogenous spectrum between the geometric and Kolmogorov scales and is approximately isotropic [7]. The turbulent intensity decays with distance downstream of the screen following a power law relationship. Therefore, by moving the mesh on its track, we varied the distance from the mesh to the Pitot tube and achieved values spanning the range from  $0.25\% < T < 2\%$ .

### 5.3. Calibrations depend on turbulence

Fig. 4 shows calibration curves for the Pitot tube oriented at 20° yaw and 0° pitch away from the tunnel's axis with different values of  $T$ . When  $T$  is greater than 1% the hysteresis is not present however; the shape of the calibration curve is  $T$ -dependent. With  $T=2\%$ , the calibration curve is approximately linear in the region near the hysteresis.

Over the whole range of  $0.25\% < T < 2\%$ , that we were able to produce, the calibration of the multi-holed tube was dependent on the turbulent intensity. The 1-D Pitot static tube that we used as a check standard (and also for the denominator in  $C_i$ ) was oriented along the flow direction during all of the calibrations and did not exhibit  $T$  dependence greater than its uncertainty.

In order to produce a relevant calibration for a multi-holed Pitot tube in the range  $20^\circ \pm 5^\circ$  away from the tunnel's axis, the turbulence level must match the level present in the flow the probe will be used.

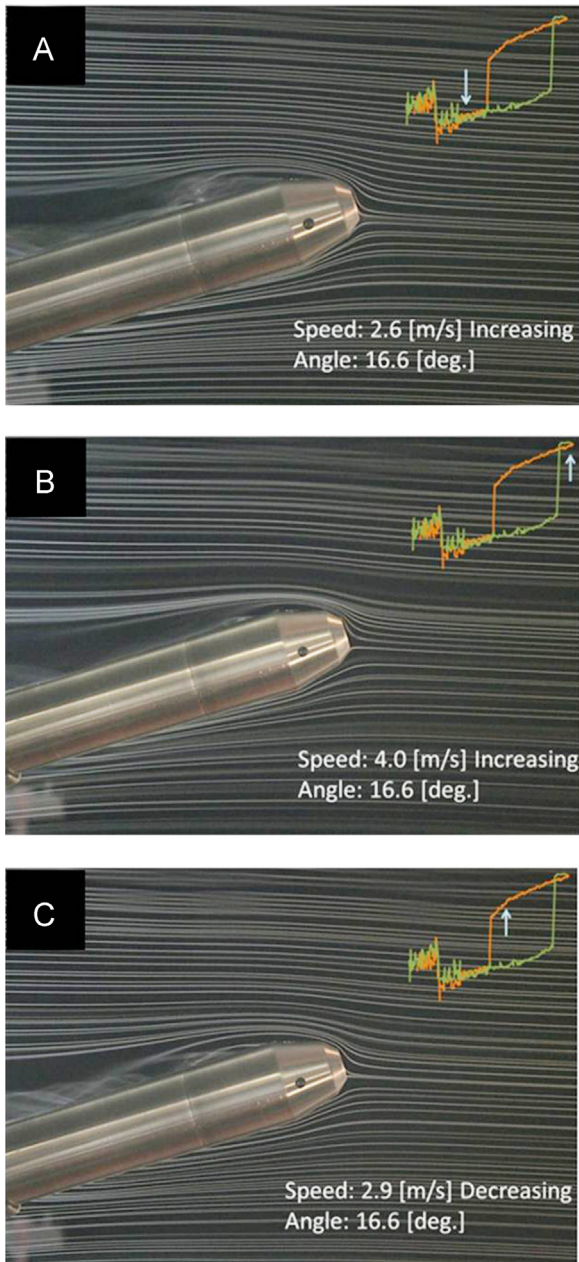


Fig. 3. Visualization of flow around the model Pitot tube. Note the strong recirculation in all three pictures.

## 6. Conclusion

Flow separation and recirculation are common phenomena; therefore, the hysteresis that we observed is likely to occur during

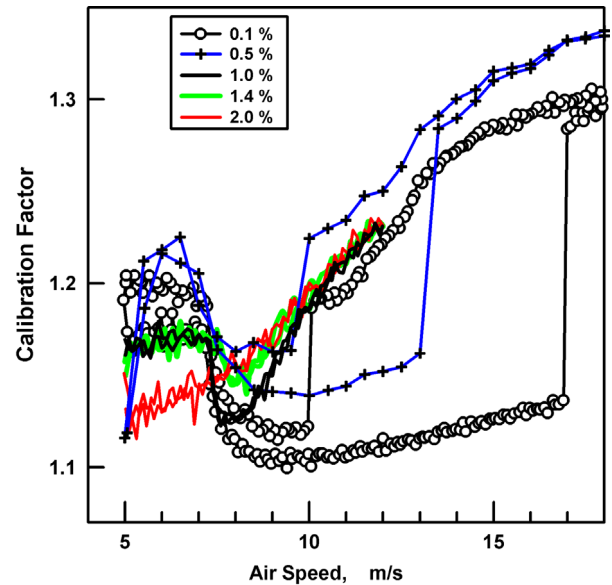


Fig. 4. Calibration of the original Pitot tube under different turbulent intensities.

the calibration of other multi-hole Pitot tubes at other pitch and yaw angles. In the case of a cone-shaped five-hole Pitot tube, the detachment of flow caused hysteresis that was observed to be as large as 30%. The structure of detached flows depends on the turbulent intensity. Therefore calibration of the multi-hole pitot tube should be performed in the range of turbulence intensities expected to be present when the calibrated instrument is used. The turbulent intensity in smokestacks, where this Pitot tubes calibration will be used, is most likely greater than 2%. Therefore, the hysteresis will not be observed due to the high level of turbulence and calibration produced in a quiet wind tunnel (less than the turbulence level in the stack) will be irrelevant in the stack. We are modifying our wind tunnel to enable calibrations of multi-hole Pitot tubes at higher turbulent intensities.

## References

- [1] Shinder II, Crowley CJ, Moldover MR. Calibrations of multi-holed Pitot tubes depend on turbulence. In: Proceeding of the MSC: Pasadena, California; 2012.
- [2] Marland G, Rotty RM. Carbon dioxide emissions from fossil-fuels: a procedure for estimation and results for 1950–1982. *Tellus Series B* 1984;36:232–61.
- [3] U.S. Energy Information Administration. Documentation for Emissions of Greenhouse Gasses in the United States 2005: EIA, Washington DC; 2007.
- [4] Bryer DW, Pankhurst RC. Pressure-probe methods for determining wind speed and flow direction; 1971.
- [5] Yeh TT, Hall MJ. Airspeed Calibration Service. NIST Special Publication SP 250-73.
- [6] Shinder II, Hall MJ, Moldover MR. Improved NIST Airspeed Calibration Facility. In: Proceeding of the MSC: Pasadena, California; 2012.
- [7] Kurian T, Fransson JHM. Grid-generated turbulence revisited. *Fluid Dynamics Research* 2009;41 UK.